ACI STRUCTURAL JOURNAL TECHNICAL PAPER

Title no. 101-S24

Strengthening of Cantilever and Continuous Beams Using New Triaxially Braided Ductile Fabric

by Nabil F. Grace, Wael F. Ragheb, and George Abdel-Sayed

This paper deals with the effectiveness of a new triaxially braided ductile fiber-reinforced polymer (FRP) fabric for flexural strengthening of cantilever and continuous reinforced concrete beams. Two series of beams were experimentally investigated. The first series included beams with one overhanging cantilever strengthened in flexure and loaded with one concentrated load at the end of the cantilever. The second series included continuous beams with two spans strengthened in flexure along their positive and negative moment regions and loaded with a concentrated load at the middle of each span. One beam in each series was not strengthened and was tested as a control beam. The behaviors of the beams strengthened with the new fabric were investigated and compared with the behaviors of similar beams strengthened using a commercially available carbon fiber sheet. The responses of the beams were examined in terms of deflections, strains, and failure modes. The beams strengthened with the new fabric showed greater ductility than those strengthened with the carbon fiber sheet. The new fabric provided reasonable ductility due to the formation of the plastic hinges that allowed for the redistribution of the moment between the positive and negative moment zones of the strengthened continuous beam. Redistribution of the moment enabled the full use of the strength of the beam at cross sections of maximum positive and negative bending moments.

Keywords: concrete; ductility; flexural strengthening; polymer.

INTRODUCTION

Ductility is an important requirement in the design of any structural element. With respect to reinforced concrete continuous beams, ductility allows the redistribution of the moment between the negative and positive moment zones. The formation of plastic hinges allows the utilization of the full capacity of more cross sections of the beams. The beam must be able to rotate adequately at the plastic hinges, however, to allow the redistribution of moment.

Fiber-reinforced polymer (FRP) materials in forms such as pultruded plates, fabrics, and sheets have been attractive for use as strengthening materials for reinforced concrete beams. A large loss in beam ductility, however, occurs when they are used for flexural strengthening of reinforced concrete beams, as reported in Saadatmanesh and Ehsani (1991), Ritchie, Thomas, and Connelly (1991), Triantafillou and Plevris (1992), Norris, Saadatmanesh, and Ehsani (1997), Arduini, Tommaso, and Nanni (1997), and Bencardino, Spadea, and Swamy (2002). The loss in beam ductility is attributed, in part, to the mechanical characteristics of these materials. Grace et al. (2002) showed that because these materials have dissimilar behavior to that of steel, that is, they exhibit a linear stress-strain behavior up to failure; they indirectly invoke brittle failures such as FRP debonding or shear-tension failure. In addition, the gain in beam yield load and stiffness after strengthening is not as significant as that of the ultimate load. Due to their high ultimate strains compared with the yield strain of steel, the FRP do not contribute with significant amounts of their strength at low strain levels such as that below the yield strain of steel.

Limited experimental investigations have been reported on the behavior of reinforced concrete beams strengthened in flexure in their negative moment regions using FRP materials. Grace et al. (1999) reported experimental investigations for reinforced concrete beams strengthened in flexure using carbon fiber reinforced polymer (CFRP) laminates. Although increases in ultimate loads were gained, large losses in ductility were experienced. The strengthened beams also showed no yield plateaus. Grace (2001) used CFRP strips to strengthen the negative moment regions of reinforced concrete cantilever beams. The strengthened beams experienced brittle failures as a result of strip debonding or shear-tension failure at the strip ends.

A new pseudo-ductile FRP strengthening fabric has been developed at the Structural Testing Center at Lawrence Technological University. The fabric is unique in that it exhibits a yield plateau similar to that exhibited by steel in tension. The fabric has a low yield-equivalent strain (0.35%) that allows it to have the potential to contribute significantly to the beam load before yielding of the steel reinforcement of the strengthened beams, and a reasonable ultimate strain (approximately 2%), that allows the strengthened beam to exhibit adequate ductility before the fabric ruptures. This fabric was manufactured by triaxially braiding bundles of carbon and glass fibers in three different directions (+45, 0, and –45 degrees). These fibers were selected with different ultimate strains (0.35, 0.8, 2.10%) and were mixed in a way allowing them to fail successively generating a yield plateau. The fabric was designed to be used for beam strengthening for flexure and/or shear. The 0 degree fibers are mainly used for flexural strengthening, while the (+45 and –45 degrees) fibers are mainly used for shear strengthening and to provide self anchoring when wrapping the beam. Figure 1 shows details of the triaxial ductile fabric geometry and Fig. 2 shows the average tensile load-strain response of samples tested in the 0 degree direction, according to ASTM D 3039 specifications. Grace, Abdel-Sayed, and Ragheb (2003) used this fabric to strengthen reinforced concrete simple beams for flexure. The beams strengthened with the new fabric behaved in a more ductile manner than those strengthened with the carbon fiber sheets. The beams strengthened with the new fabric produced yield plateaus similar to that of the unstrengthened beam and also similar to those produced by beams strengthened with steel plates. In this paper, the effectiveness of this fabric in

ACI Structural Journal, V. 101, No. 2, March-April 2004.
MS No. 02-463 received December 9, 2002, and reviewed under Institute publication policies. Pertinent discussion including author's closure, if any, will be published in the January-February 2005 *ACI Structural Journal* if the discussion is received by September 1, 2004.

ACI member **Nabil F. Grace** *is a professor and Chair of the Department of Civil Engineering, Lawrence Technological University, Southfield, Mich. He is a member of ACI Committee 440, Fiber Reinforced Polymer Reinforcement, and Joint ACI-ASCE Committee 343, Concrete Bridge Design.*

Wael F. Ragheb *received his PhD from the University of Windsor, Windsor, Ontario, Canada. His research interests include the use of hybrid FRP in reinforced concrete structures.*

George Abdel-Sayed *is Professor Emeritus, Department of Civil and Environmental Engineering, University of Windsor, Windsor, Ontario, Canada.*

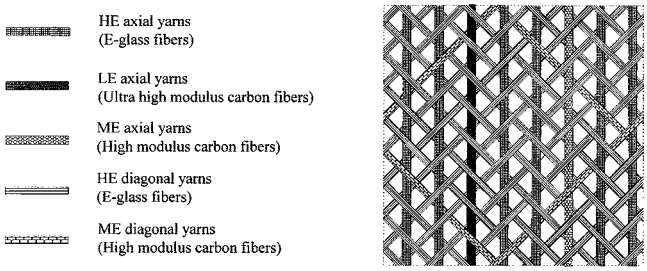

Fig. 1—Details of triaxial ductile fabric geometry.

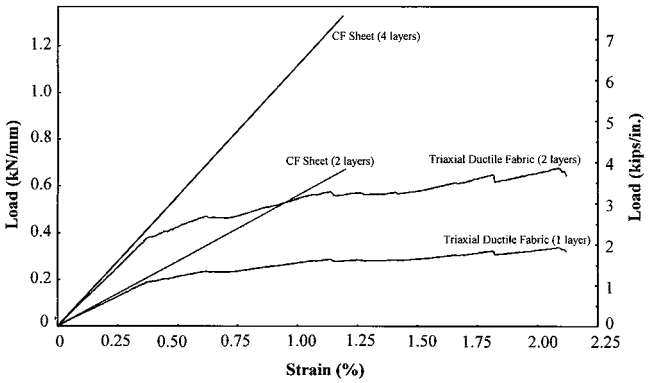

Fig. 2—Tensile properties of materials used.

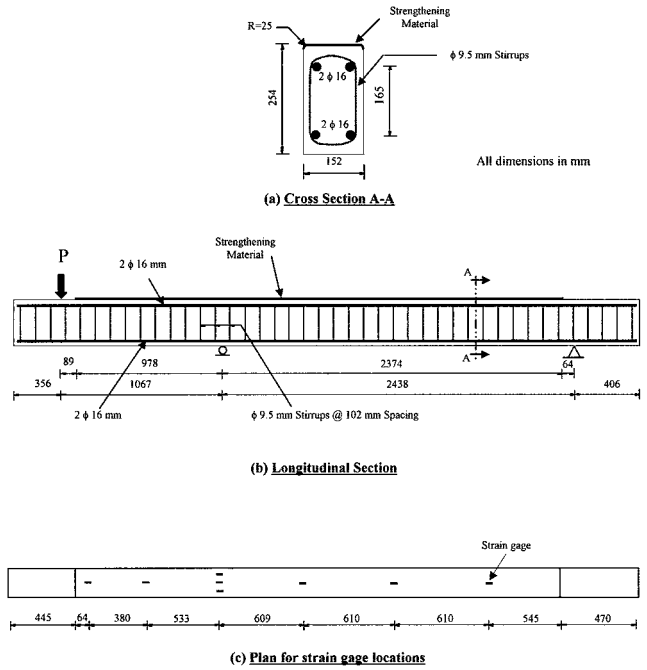

Fig. 3—Test beam details of Series A.

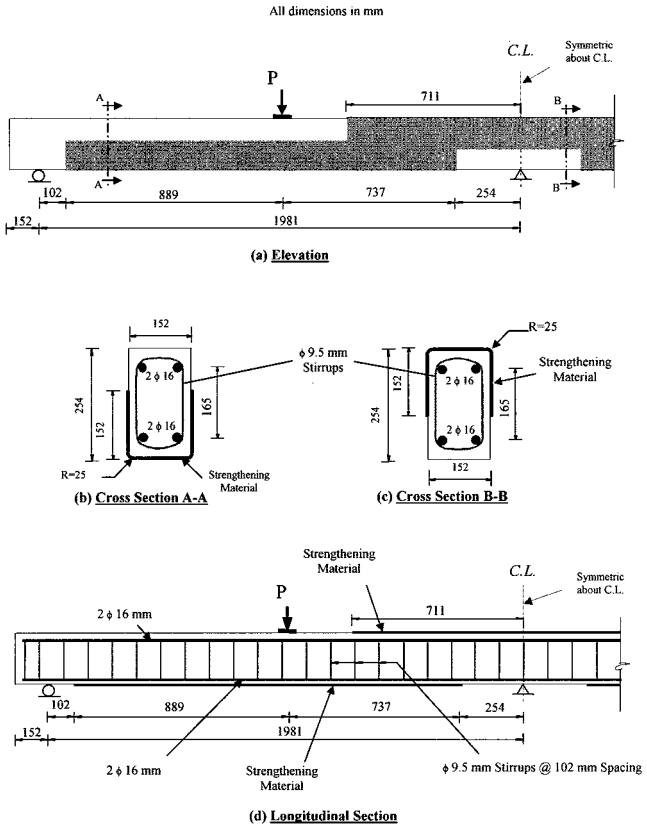

Fig. 4—Test beam details of Series B.

providing ductile behaviors in reinforced concrete continuous and cantilever beams strengthened in flexure is investigated.

RESEARCH SIGNIFICANCE

Ductility is a very important requirement in the design of structural elements. Ductile structures can exhibit large deformations before any potential failure and thus provide visual indicators that give the opportunity for remedial actions prior to failure. Ductility is even more important for statically indeterminate structures, such as continuous beams, as it allows for moment redistribution through the rotations of plastic hinges. Moment redistribution permits the utilization of the full capacity of more segments of the beam. A large loss in ductility is experienced when using currently available FRP materials for strengthening reinforced concrete beams for flexure. This paper investigates the capability of a new triaxial ductile FRP fabric to offer adequate ductility at the plastic hinge regions of strengthened reinforced concrete cantilever and continuous beams in flexure.

EXPERIMENTAL PROGRAM

Test beams

The experimental program consisted of testing two beam series with three beams each. All beams had identical cross sectional dimensions of 152 x 254 mm (6 x 10 in.) and lengths of 4267 mm (168 in.). The beams were symmetrically reinforced with two No. 5 (ϕ 16 mm) rods at the top and the bottom. To avoid shear failure, the beams were over-reinforced for shear with No. 3 (ϕ 9.5 mm) closed stirrups spaced at 102 mm (4.0 in.). The beams of the first series, Series A, were tested with one overhanging cantilever, while the beams of the second series, Series B, were tested with two continuous spans. Figure 3 and 4 show the beam dimensions,

Table 1—Properties of strengthening materials

Type	Yield-equivalent load, kN/mm (kips/in.)	Yield-equivalent strain, %	Ultimate load, kN/mm (kips/in.)	Ultimate strain, %	Thickness, mm (in.)
Carbon fiber sheet	—	—	0.34 (1.95)	1.2	0.13 (0.005)
Triaxial ductile fabric	0.19 (1.08)	0.35	0.33 (1.89)	2.10	1.0 (0.039)

reinforcement details, and loading setup of Series A and B, respectively. The beams were prepared by sandblasting their surfaces to roughen them, cleaned with an air nozzle, and finally wiped to remove any dust. The compressive strength of the concrete at the time the beams were tested was 41.5 MPa (6000 psi). The steel reinforcement used had a yield stress of 490 MPa (71,000 psi).

Strengthening materials

In addition to the new triaxial ductile fabric, a commercially available carbon fiber sheet was used to strengthen similar beams to compare their behavior with those strengthened with the new fabric. To have an objective comparison, the carbon fiber sheet was selected to have a similar load-strain response to that initially exhibited by the triaxial ductile fabric (before exceeding its yield-equivalent point). The tested load-strain diagrams of the triaxial ductile fabric and the carbon fibers sheet are shown in Fig. 2 and their properties are listed in Table 1. Herein, it can be noted that the triaxial ductile fabric has a yield-equivalent load of 0.19 kN/mm (1.08 kips/in.), while the carbon fiber sheet has an ultimate load of 0.34 kN/mm (1.95 kips/in). Using the tensile properties of the materials, it was determined that two layers of the carbon fiber sheet would exhibit a load-strain response similar to that initially exhibited by one layer of the triaxial ductile fabric. An epoxy resin was used to impregnate the fibers and to act as an adhesive between the strengthening material and the concrete surface. This epoxy has an ultimate tensile strength of 66.2 MPa (9.62 ksi) with an ultimate strain of 4.4% and a compressive strength of 109.2 MPa (15.84 ksi).

Strengthening and setup

Series A—Series A consisted of three beams with one overhanging cantilever each. Each beam had an inner span of 2438 mm (96 in.) and a cantilever span of 1067 mm (42 in.). One of these beams had no external strengthening and was tested as a control beam. The other two beams were strengthened on their top faces along 3352 mm (132 in.) of their lengths, as shown in Fig. 3. One of these two beams, Beam F-NV, was strengthened using two layers of the triaxial ductile fabric that were each 135 mm (5.33 in.) wide. The other beam, Beam F-NVC, was strengthened using four layers of the carbon fiber sheet that were each 146 mm (5.75 in.) wide. The deflection of the cantilever was measured at the loading point and at its midspan, while the deflection of the inner span was measured at its mid and quarter points, using string potentiometers. The FRP strain was measured at different locations along the beam using electrical resistance strain gages, as shown in Fig. 3(c). The beams were loaded using a hydraulic actuator.

Series B—Series B consisted of three continuous beams. Each beam had two spans of 1981 mm (78 in.) each. The beams were loaded with a concentrated load at the middle of each span. One of these beams had no external strengthening and was tested as a control beam. The other two beams were strengthened along their negative and positive moment regions around the top/bottom face extending 152 mm (6 in.) on both sides as a U-wrap at the locations shown in Fig. 4. The first beam, Beam F-CT, was strengthened using one layer of the triaxial ductile fabric that was 457 mm (18 in.) wide, U-wrapped around the tension faces and the sides, while the other beam, Beam F-CTC, was strengthened using two layers of the carbon fiber sheet that were each 457 mm (18 in.) wide, with the same wrapping scheme. The deflection was measured at the middle and quarter of each span using string potentiometers. The FRP strain was measured at the beam tension face at the central support and at the middle of each span using electrical resistance strain gages. The reaction of the beam at the central support was measured using a load cell. Two hydraulic actuators were used to load the beam, one for each span. The load of each actuator was measured using a load cell. Table 2 summarizes the test beams.

Table 2—Summary of test beams

Beam series	Beam designation	Strengthening scheme	Strengthening material	Positive moment strengthening		Negative moment strengthening	
				No. of layers	Strengthened length	No. of layers	Strengthened length
Series A	Control A	N/A	N/A	None	None	None	None
	F-NV	Tension face only	Triaxial ductile fabric	None	None	2	3.35 m (11 ft)
	F-NVC		Carbon fiber sheet	None	None	4	
Series B	Control B	N/A	N/A	None	None	None	None
	F-CT	U-wrap around tension face and sides	Triaxial ductile fabric	1	1.63 m (5.33 ft)	1	1.42 m (4.67 ft)
	F-CTC		Carbon fiber sheet	2		2	

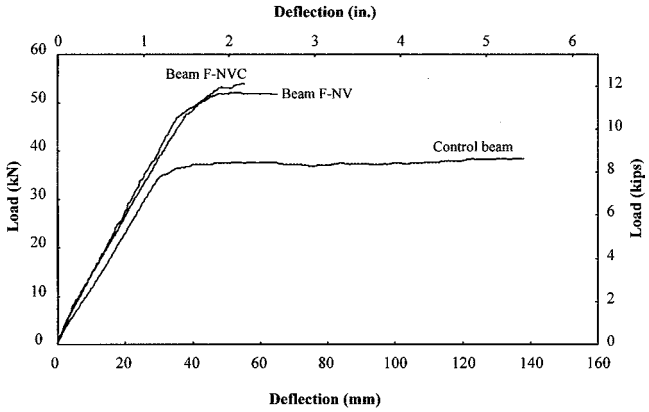

Fig. 5—Load-cantilever end deflection curves of Series A beams.

TEST RESULTS AND DISCUSSION

Series A

Test results for Series A beams are shown Fig. 5 to 8 and listed in Table 3. The failed beams are shown in Fig. 9 to 11. The ductility of each beam was determined by calculating its ductility index; that is, the ratio between the ultimate deflection and the yield deflection of the cantilever end at the loading point.

Control Beam A—The control beam had a yield load of 35 kN (7.9 kips) and an ultimate load of 38 kN (8.5 kips). The beam

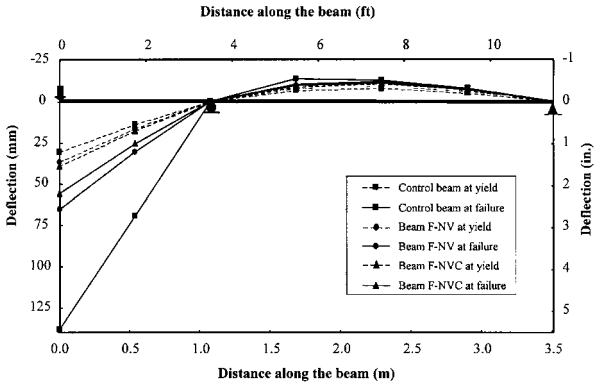

Fig. 6—Deflection profiles of Series A beams.

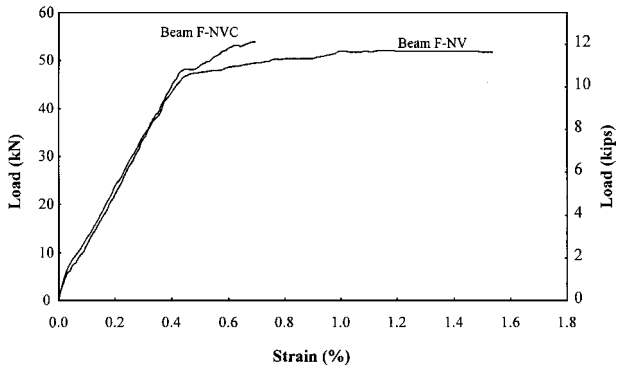

Fig. 7—FRP strain at section of maximum bonding moment.

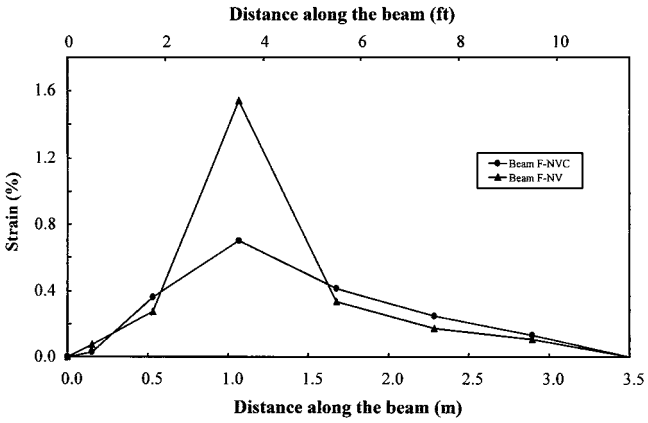

Fig. 8—FRP strain profiles at failure of Series A beams.

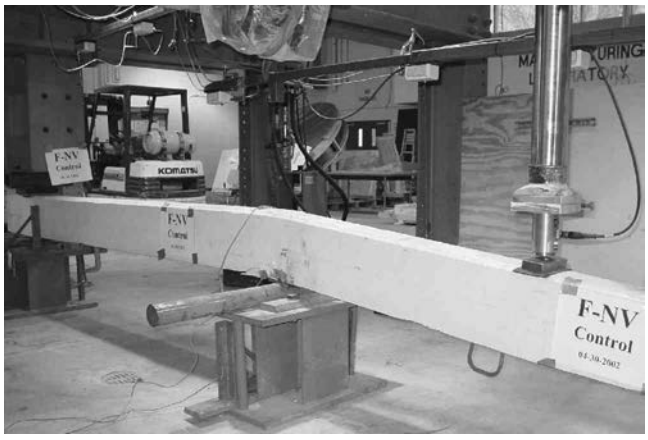

Fig. 9—Failure of control Beam A.

Fig. 10—Failure of Beam F-NV.

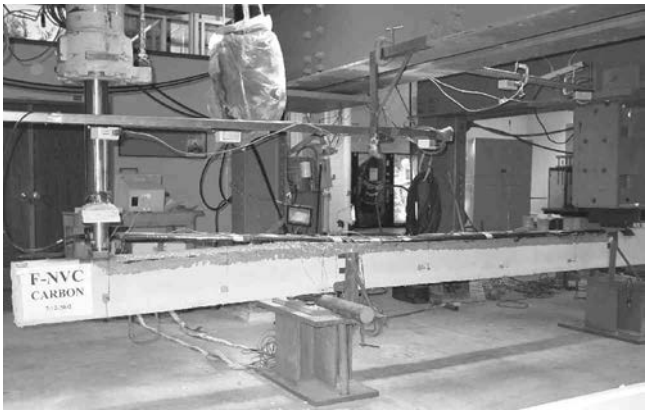

Fig. 11—Failure of Beam F-NVC.

failed by yielding of steel followed by compression failure of concrete at the section of maximum bending moment. Figure 5 indicates that the cantilever end exhibited excessive deflections after yielding with a considerable yield plateau. The beam had a ductility index of 4.53. The failed beam is shown in Fig. 9. The deflection profile shown in Fig. 6 indicates that a considerable rotation of the beam occurred after the formation of the plastic hinge.

Beam F-NV—Beam F-NV yielded at a load of 47 kN (10.6 kips) due to yielding of both the steel and the fabric. The fabric yield was accompanied by the sounds of ruptures of its low elongation fibers. Failure in Beam F-NV occurred at a load of 52 kN (11.7 kips) due to rupture of the fabric. A ductility index of 1.83 was exhibited, which was 60% less than that of the control beam. The fabric showed a considerable increase in strain after yield, as shown in Fig. 7. The fabric strength was fully exploited, as its maximum recorded strain was 1.54%, which was more than its yield-equivalent strain. The strain profile at failure, shown in Fig. 8, shows a noticeable increase in fabric strain at the section of the maximum bending moment. The failed beam is shown in Fig. 10.

Beam F-NVC—Beam F-NVC behaved similarly to Beam F-NV up to yield, which occurred due to yielding of the steel reinforcement at a load of 48 kN (10.8 kips) and failed suddenly at a load of 54 kN (12.1 kips) due to debonding of the carbon fiber sheet from the concrete surface. The beam showed almost no yield plateau with a ductility index of 1.47, which was 68% less than that of the control beam. The

Table 3—Summary of test results

Beam series	Beam designation	Strengthening system	Yield load, kN (kips)	Deflection* at yield, mm (in.)	Failure load, kN (kips)	Deflection* at failure, mm (in.)	Middle support reaction at failure, kN (kips)	Maximum negative moment at failure,† kN.m (kips.in.)	Maximum negative moment based on elastic analysis,‡ kN.m (kips.in.)	Moment redistribution ratio, % = (Col. 9 – Col. 8)/ (Col. 9)%	Ductility index = (Col. 6)/ (Col. 4)	Type of final failure
	(1)	(2)	(3)	(4)	(5)	(6)	(7)	(8)	(9)	(10)	(11)	(12)
Series A	Control A	N/A	35 (7.9)	30.5 (1.20)	38 (8.5)	138.2 (5.44)	N/A	N/A	N/A	N/A	4.53	Steel yield followed by concrete failure
	F-NV	Triaxial ductile fabric	47 (10.6)	35.7 (1.41)	52 (11.7)	65.3 (2.57)	N/A	N/A	N/A	N/A	1.83	Steel and fabric yield followed by fabric rupture
	F-NVC	Carbon fiber sheet	48 (10.8)	37.8 (1.49)	54 (12.1)	55.6 (2.19)	N/A	N/A	N/A	N/A	1.47	Steel yield followed by sheet debonding
Series B	Control B	N/A	92 (20.7)	9.3 (0.37)	127 (28.5)	29.1 (1.15)	168 (37.8)	40.6 (359)	47.3 (418)	14.2	3.12	Steel yield followed by concrete failure
	F-CT	Triaxial ductile fabric	126 (28.3)	9.1 (0.36)	175 (39.3)	23.4 (0.92)	232 (52.1)	56.4 (499)	65.1 (575)	13.4	2.57	Steel and fabric followed by fabric rupture
	F-CTC	Carbon fiber sheet	136 (30.6)	8.9 (0.35)	185 (41.6)	16.1 (0.63)	250 (56.2)	64.4 (569)	68.9 (609)	6.5	1.81	Steel yield followed by shear-tension failure at sheet end

Note: Col. = Column.
*Deflection at loading point(s).
†Based on loads and reactions in Columns (5) and (7).
‡Equal to 0.188 × load × beam span.

maximum recorded carbon fiber strain at the section of the maximum bending moment was 0.70%, indicating that only 58% of the sheet strength was used. Figure 8 shows that the strain distribution along the beam at failure was very similar to the distribution of the bending moment. Figure 11 shows the failed beam.

Clearly, the difference between the failure modes of Beam F-NV and F-NVC can be attributed to the difference in the tensile behavior between the triaxial ductile fabric and the carbon fiber sheet. While the carbon fiber sheet exhibits a linear stress-strain response up to failure, the triaxial ductile fabric exhibits a linear stress-strain behavior up to a certain point, where the strain increases without a similar increase in load. Because the four layers of the carbon fiber sheet used in Beam F-NVC had similar load-strain behavior to that initially provided by the two layers of the triaxial ductile fabric used in Beam F-NV, Beam F-NVC behaved similarly to Beam F-NV up to yield. After yield, the two beams behaved differently. The tension force in the carbon fiber sheet kept increasing after yielding of Beam F-NVC, exceeding its anchorable limit and causing debonding of the sheet from the concrete surface. On the other hand, the force in the triaxial ductile fabric used in Beam F-NV did not significantly increase after it yielded. Thus, it did not exceed its anchorable limit and debonding did not take place. In addition, the triaxial ductile fabric exhibited an increase in strain after yield, which resulted in a higher ductility.

Series B

Test results for the beams of this series are shown Fig. 12 to 15, and listed in Table 3. The failed beams are shown in

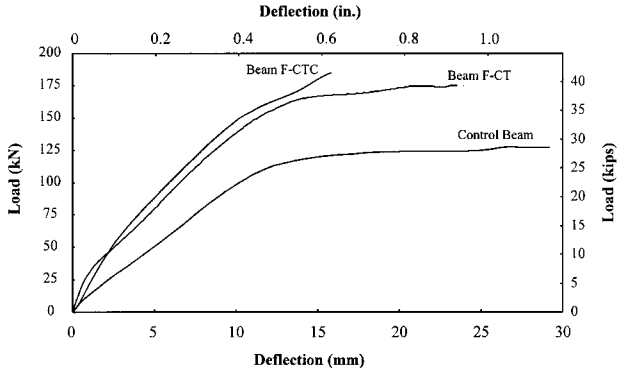

Fig. 12—Load-midspan deflection curves of Series B beams.

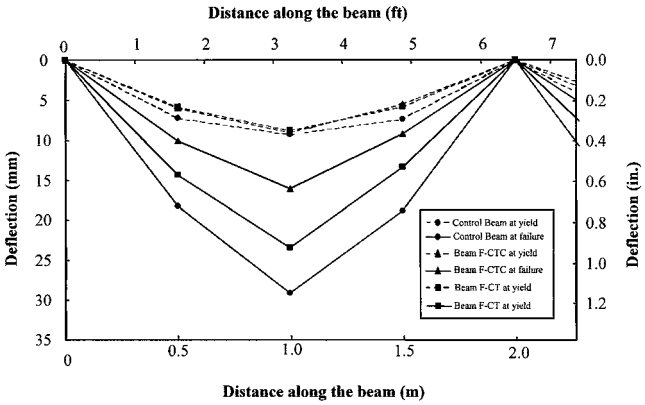

Fig. 13—Deflection profile of Series B beams.

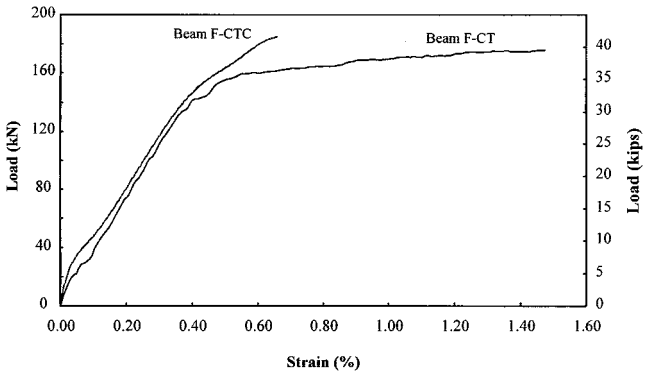

Fig. 14—FRP strain at midspan of Series B beams.

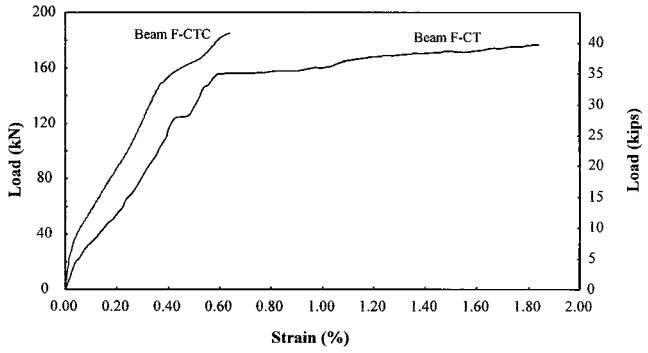

Fig. 15—FRP strain at central support of Series B beams.

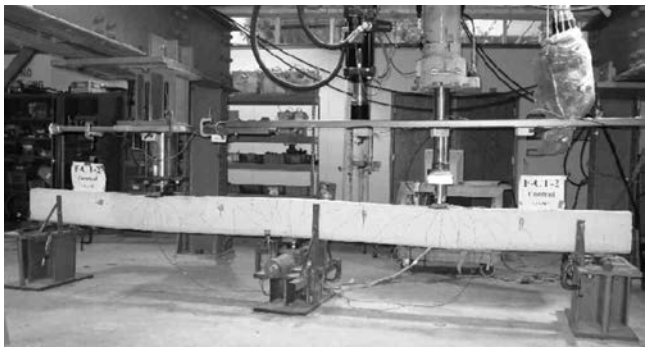

Fig. 16—Control Beam B at failure.

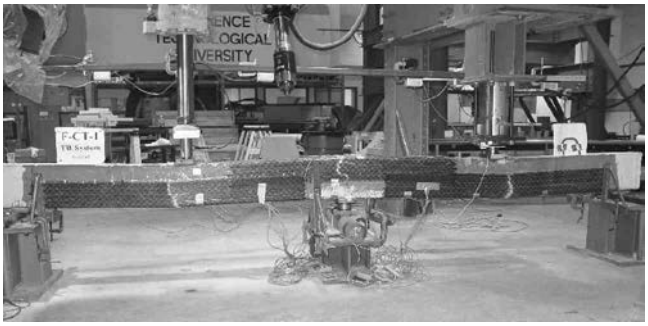

Fig. 17—Beam F-CT at failure.

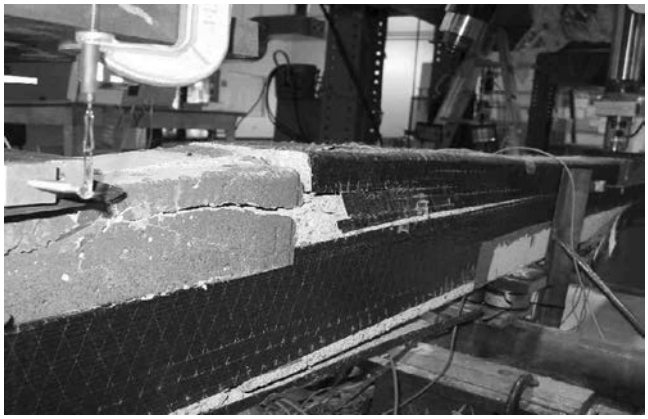

Fig. 18—Shear-tension failure at sheet end of Beam CTC.

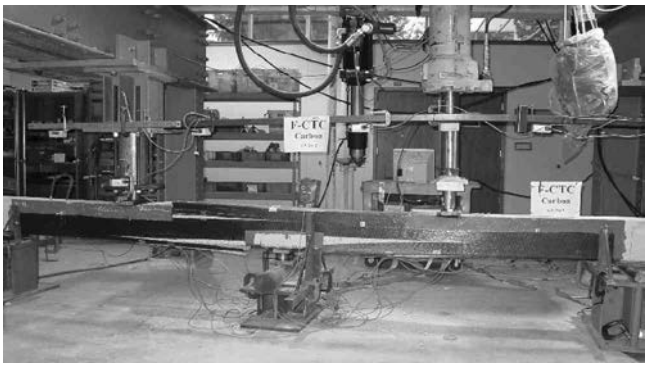

Fig. 19—Beam F-CTC at failure.

Fig. 16 through 19. Note that the load in Fig. 12, 14, and 15 is the load at each span *P* and not the total load on the beam. The beam ductility index is calculated as the ratio between the ultimate midspan deflection and its deflection at first yield.

Control Beam B—The control beam exhibited a linear load-deflection behavior after cracking up to yielding of the tension steel at the section of the maximum negative bending moment over the central support, which occurred at a load of 92 kN (20.7 kips). After this point, a gradual decrease in the slope of the load-deflection curve was observed. The tension steel at the sections of the maximum positive bending moment yielded later, causing a significant decrease in beam stiffness as the deflection then started to increase significantly without a corresponding increase in load, as shown in Fig. 12. The beam failed by compression failure of the concrete at the midspan at a load of 127 kN (28.5 kips). A ductility index of 3.12 was observed. The beam deflection profile, shown in Fig. 13, indicates that deformation of the beam at failure was very localized at the sections of maximum positive and negative moments, at the midspan and the central support, respectively.

Beam F-CT—Beam F-CT yielded at a load of 126 kN (28.3 kips) due to yielding of both the tension steel and the fabric over the central support. Yielding of the fabric was accompanied by the sounds of rupture of the low elongation fibers of the fabric. A gradual decrease in beam stiffness was observed, which was revealed by the decrease in the slope of the load-deflection curve, as shown in Fig. 12. A significant decrease in beam stiffness was observed after yielding of the beam at the sections of maximum positive moment, which was caused by yielding of both the tension steel and the fabric. A yield plateau similar to that exhibited by the control beam was exhibited thereafter until failure at a load of 175 kN (39.2 kips). The beam failed by tensile rupture of the fabric over the central support, followed by rupture of the fabric at midspan (refer to Fig. 17). A ductility index of 2.57 was

exhibited, which was 18% less than that of the control beam. The load-strain diagrams of the fabric at the midspan and over the central support are shown in Fig. 14 and 15, respectively. At first failure, the fabric exhibited strain values of 1.8 and 1.47% at the sections of maximum negative and positive moments, respectively. The fact that these strain values were more than the yield-equivalent strain of the fabric indicated that fabric strength was exploited.

Beam F-CTC—Beam F-CTC yielded at a load of 136 kN (30.6 kips), where a slight decrease in the load-deflection curve slope was exhibited caused by yielding of the tension steel at the section of the maximum negative moment over the central support. The beam exceeded the load achieved by Beam F-CT and failed suddenly at a load of 185 kN (41.6 kips) by shear-tension failure at one end of the negative moment strengthening carbon fiber sheet, as shown in the photo in Fig. 18, followed by debonding of the carbon fiber sheet of the positive moment, as shown in Fig. 19. A ductility index of 1.81 was observed, which was 42% less than that of the control beam. The load-deflection curve indicates a very brittle response as shown in Fig. 12. No significant yield plateau was experienced. The load-strain curves, shown in Fig. 14 and 15, indicate that the carbon fiber sheet exhibited noticeably less strain than the triaxial ductile fabric used in Beam F-CT. The maximum recorded strain values did not exceed 0.66%, which indicated that nearly half the strength of the carbon fiber sheet was not exploited.

The new triaxial ductile fabric contains bundles of fibers in the ±45 degree directions. These fibers enable the fabric to have a self-anchorage along its length, when U-wrapped around the tension face and the vertical sides of the beam. As a result, anchorage failures similar to those experienced by Beam F-CTC were not experienced in case of Beam F-CT. On the other hand, the carbon fiber sheet used in Beam F-CTC is uniaxial, and hence wrapping the beam did not enhance the anchorage. In addition, yielding of the fabric limited the increase in the tensile force developed in it. Therefore, the fabric needed less anchorage than the carbon fiber sheet, whose tensile force kept increasing until a brittle failure took place.

Using the readings of the load cell located at the central support, the actual bending moment diagram for each beam at failure was determined. Also, the bending moment diagram based on elastic analysis was determined for each beam using the value of the failure load. This is shown in Fig. 20. It is clear from the figure that unlike Beam F-CTC, Beam F-CT exhibited a similar level of moment redistribution to that of the control beam. The moment redistribution ratio shown in Table 3 was calculated for each beam by calculating the value of the maximum negative moment, based on the elastic analysis, and comparing it with the experimental value at beam failure. Beam F-CT had a redistribution ratio of 13.4%, which was 6% less than that of the control beam. On the other hand, Beam F-CTC had a redistribution ratio of 6.5%, which was significantly less than that of Beam F-CT. The ductile behavior of the new fabric resulted in a reasonable ductility in the plastic hinge regions in Beam F-CT, which in turn allowed for the redistribution of moment between positive and negative moment zones.

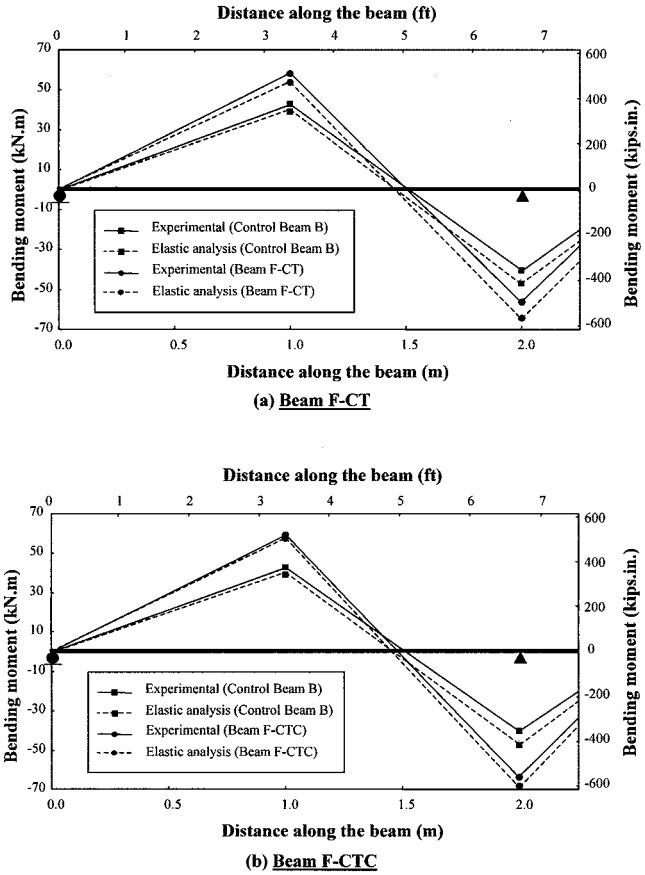

Fig. 20—Elastic and experimental bending moment diagrams at failure for Series B beams.

CONCLUSIONS

1. The unique characteristics of the new triaxial ductile fabric helped to reduce the significant loss in beam ductility associated with the use of conventional FRP materials in flexural strengthening of reinforced concrete beams. The beams strengthened with the new fabric exhibited 24 to 42% higher ductility index than those strengthened with the carbon fiber sheet;

2. The triaxial ductile fabric was successful in providing reasonable ductility at the plastic hinge regions. Therefore, the redistribution of the moment between the negative and positive moment zones of the continuous beam became possible. Redistribution of the moment allowed full use of the strength of the beam at the cross sections of maximum positive and negative moments;

3. Yielding of the triaxial ductile fabric was accompanied by various noticeably audible sounds for a long period of time that were loud enough to be considered as a warning sign;

4. The beams strengthened with the triaxial ductile fabric did not exhibit anchorage failures. That is attributed, in part, to its ductile behavior. The force in the fabric did not significantly increase after it yielded. Thus, it did not exceed its anchorable force limit and debonding did not take place;

5. The existence of bundles of fibers in the ±45 degree directions enable the triaxial ductile fabric to "self anchor" when wrapped around the tension face and the vertical sides of the beam along its length. Therefore, it was generally less vulnerable to anchorage failures than the uniaxial carbon fiber sheet; and

6. The strength of the triaxial ductile fabric was fully exploited as its maximum recorded strains before beam failure were much more than its yield-equivalent strain. In contrast, the maximum recorded strains of the carbon fiber sheet were noticeably less than its ultimate strain, which indicated that its strength was not fully exploited.

ACKNOWLEDGMENTS

This research has been conducted at the Structural Testing Center at Lawrence Technological University, Southfield, Mich., and was funded by the National Science Foundation under Grant No. CMS-9906404, awarded to the first author. The features of the developed triaxially braided ductile fabric, as well as certain applications for the fabric, are the subject of a pending U.S. patent application. The authors wish to thank Diversified Composites Inc., Erlanger, Ky., for manufacturing the fabric, Shelby Precast Concrete, Shelby Township, Mich., for contributing the test beams, and Baker Concrete Technology Inc., Columbus, Ohio, for contributing the carbon fiber sheet used.

REFERENCES

Arduini, M.; Tommaso, A. D.; and Nanni, A., 1997, "Brittle Failure in FRP Plate and Sheet Bonded Beams," *ACI Structural Journal*, V. 94, No. 4, Jul.-Aug., pp. 363-370.

ASTM D 3039, 2000, "Standard Test Method for Tensile Properties of Polymer Matrix Composite Materials," *Annual Book of ASTM Standards*, ASTM, V. 15.03, pp. 106-118.

Bencardino, F.; Spadea, G.; and Swamy, N., 2002, "Strength and Ductility of Reinforced Concrete Beams Externally Reinforced with Carbon Fiber Fabric," *ACI Structural Journal*, V. 99, No. 2, Mar.-Apr., pp. 163-171.

Grace, N. F., 2001, "Strengthening of Negative Moment Region of Reinforced Concrete Beams Using Carbon Fiber-Reinforced Polymer Strips," *ACI Structural Journal*, V. 98, No. 3, May-June, pp. 347-358.

Grace, N. F.; Abdel-Sayed, G.; and Ragheb, W. F., 2003, "Flexural and Shear Strengthening of Concrete Beams Using New Triaxially Braided Ductile Fabric," *ACI Structural Journal*, V. 100, No. 6, Nov.-Dec., pp. 804-814.

Grace, N. F.; Soliman, A. K.; Abdel-Sayed, G.; and Saleh, K. R., 1999, "Strengthening of Continuous Beams Using Fiber Reinforced Polymer Laminates," *Fourth International Symposium on Fiber Reinforced Polymer for Reinforced Concrete Structures*, SP-188, C. W. Dolan, S. H. Rizkalla, and A. Nanni, eds., American Concrete Institute, Farmington Hills, Mich., pp. 647-657.

Norris, T.; Saadatmanesh, H.; and Ehsani, M. R., 1997, "Shear and Flexural Strengthening of R/C Beams with Carbon Fiber Sheets," *Journal of Structural Engineering*, ASCE, V. 123, No. 7, pp. 903-911.

Ritchie, P. A.; Thomas, D. A.; Lu, L.; and Connelly, G. M., 1991, "External Reinforcement of Concrete Beams Using Fiber Reinforced Plastics," *ACI Structural Journal*, V. 88, No. 4, July-Aug., pp. 490-500.

Saadatmanesh, H., and Ehsani, M. R., 1991, "RC Beams Strengthened with GFRP Plates I: Experimental Study," *Journal of Structural Engineering*, ASCE, V. 117, No. 11, pp. 3417-3433.

Triantafillou, T. C., and Plevris, N., 1992, "Strengthening of RC Beams with Epoxy-Bonded-Fiber-Composite Materials," *Materials and Structures*, V. 25, pp. 201-211.